

**The hardest X-ray source in the *ASCA* Large Sky Survey:
Discovery of a new type 2 Seyfert**

Masaaki Sakano¹, Katsuji Koyama², Takeshi Tsuru² and Hisamitsu Awaki²
Department of Physics, Kyoto University, Kyoto 606-8502 Japan,
sakano@cr.scphys.kyoto-u.ac.jp, koyama@cr.scphys.kyoto-u.ac.jp,
tsuru@cr.scphys.kyoto-u.ac.jp, awaki@cr.scphys.kyoto-u.ac.jp

Yoshihiro Ueda and Tadayuki Takahashi
Institute of Space and Astronautical Science, Kanagawa 229-8510 Japan,
ueda@astro.isas.ac.jp, takahasi@astro.isas.ac.jp

Masayuki Akiyama¹ and Kouji Ohta
Department of Astronomy, Kyoto University, Kyoto 606-8502 Japan,
akiyama@kusastro.kyoto-u.ac.jp, ohta@kusastro.kyoto-u.ac.jp

and

Toru Yamada
Astronomical Institute, Tohoku University, Sendai 980-8578 Japan,
yamada@astr.tohoku.ac.jp

Received 1997, Dec 15; accepted 1998, Apr 1

¹Research Fellow of the Japan Society for the Promotion of Science.

²CREST: Japan Science and Technology Corporation (JST)

ABSTRACT

We present results of *ASCA* deep exposure observations of the hardest X-ray source discovered in the *ASCA* Large Sky Survey (LSS) project, designated as AX J131501+3141. We extract its accurate X-ray spectrum, taking account of the contamination from a nearby soft source (AX J131502+3142), separated only by $1'$. AX J131501+3141 exhibits a large absorption of $N_{\text{H}} = (6_{-2}^{+4}) \times 10^{22}$ H cm^{-2} with a photon index $\Gamma = 1.5_{-0.6}^{+0.7}$. The 2–10 keV flux was about 5×10^{-13} $\text{erg cm}^{-2} \text{ s}^{-1}$ and was time variable by a factor of 30% in 0.5 year. From the highly absorbed X-ray spectrum and the time variability, as well as the results of the optical follow-up observations (Akiyama et al. 1998), we conclude that AX J131501+3141 is a type 2 Seyfert galaxy. Discovery of such a low flux and highly absorbed X-ray source could have a significant impact on the origin of the cosmic X-ray background.

Subject headings: cosmology: diffuse radiation — galaxies: active — galaxies: individual (AX J131501+3141) — galaxies: Seyfert — X-rays: galaxies

1. Introduction

Since the discovery of the Cosmic X-Ray Background (CXB) more than 30 years ago (Giacconi et al. 1962), its origin has been a long standing puzzle. With the *ROSAT*, $\sim 70\%$ of the CXB below 2 keV has been resolved into point sources, more than 60% of which are type 1 active galactic nuclei (AGNs) (Vikhlinin et al. 1995; Hasinger 1996; McHardy et al. 1998; Hasinger et al. 1998). Origin of the CXB above the 2 keV band, however, is less clear due to the absence of the imaging instrument in this energy band. One problem in the hard X-ray band, often referred as the spectral paradox (e.g. Fabian & Barcons 1992), is that the X-ray spectrum of the CXB in the 2–10 keV band is harder than that of the typical type 1 AGN, which is presumably the main contributor to the CXB below 2 keV. The 2–10 keV X-ray spectra of type 1 Seyfert galaxies (most of the bright AGNs) are approximated by a power-law with a mean photon index of 1.7 (Mushotzky 1993), which is significantly steeper than that of the 2–10 keV CXB of about 1.4 (Gendreau et al. 1995). This fact implies that the origin of the CXB above 2 keV differs, at least in part, from that below 2 keV. In addition, 20% of the total energy of the CXB is contained in the 2–10 keV band, whereas only a few percent of the CXB is contained below 2 keV (see review by Fabian & Barcons (1992), Hasinger (1996)). Thus, the 2–10 keV band would be an essential energy range to solve the origin of the CXB.

ASCA is the first satellite with the capability of the hard X-ray (up to 10keV) imaging and spectroscopy, hence is presently the best satellite to investigate the CXB in the 2–10 keV band. In the *ASCA* Large Sky Survey project (LSS: Inoue et al. 1996; Ueda et al. 1998a), a continuous field of 7 deg² near the north galactic pole was surveyed with a sensitivity higher than any previous surveys in this energy band. Ueda et al. (1998a) resolved a significant fraction of the CXB, about 30% of the CXB, into discrete sources at a sensitivity limit of $F_X \sim 10^{-13}$ erg cm⁻² s⁻¹ (2–10 keV). The mean photon index in the 2–10 keV band for these resolved sources ($F_X = (1-4) \times 10^{-13}$ erg cm⁻² s⁻¹ in 2–10 keV) was found to be $\Gamma = 1.5 \pm 0.2$. This result is consistent with the idea that the photon index approaches to that of the CXB, $\Gamma \sim 1.4$, as the source flux decreases. However, due to limited photon statistics, the spectral information of the resolved sources was too poor to address the nature of individual X-ray sources.

The hardest source in the LSS (hereafter we refer it as the “LSS hardest source”) was found to show a photon index of $\Gamma \sim -0.2$ with no correction of an absorption (Ueda 1996). However, it is unclear whether the apparent hard spectrum is due to a large absorption or due to flatness of the intrinsic spectrum. The LSS hardest source, which was found in an unbiased survey, would provide us a good opportunity to investigate the nature of faint and hard sources which could significantly contribute to the CXB above 2 keV. Hence, we have performed follow-up *ASCA* and optical observations on the LSS hardest source. This paper reports results of the *ASCA* deep exposure observations, while those of the optical observations are given by Akiyama et al. (1998).

2. Observations and Data Reductions

We have made two follow-up *ASCA* observations of the LSS hardest source: on 1995 December 23–24 for approximately 51,000 seconds and on 1996 June 6–8 for approximately 49,000 seconds. *ASCA* has four X-ray telescopes (XRT) with focal plane detectors of two Solid State Imaging Spectrometers (SIS0 and 1) and two Gas Imaging Spectrometers (GIS2 and 3). Details of these instrumentation are found in Serlemitsos et al. (1995), Burke et al. (1991, 1994), Ohashi et al. (1996), Makishima et al. (1996), while a general description of *ASCA* can be found in Tanaka, Inoue, & Holt (1994). The observation modes were 1-CCD FAINT mode and PH nominal mode for SISs and GISs, respectively. Data reduction and cleaning were made with the standard method (Day et al. 1995).

3. Results and Analysis

3.1. X-ray Images

The LSS hardest source was detected in both the observations. Fig. 1 shows the SIS image obtained from the 2nd observation (a) in the soft band (0.5–2 keV) and (b) in the hard band (2–10 keV). The images are the sums of data from SIS0 and SIS1, smoothed with a Gaussian of $\sigma = 20$ pixels (0.54 arcmin). One point-like source is clearly seen in the 2–10 keV band image, which corresponds to the LSS hardest source. On the other hand, in the 0.5–2 keV band image, we detected another point-like source whose position shifts by about $1'$ north from the peak found in the 2–10 keV band image, but found no significant emission at the position of the LSS hardest source. The relative accuracy of the peak position of *ASCA* mainly depends on photon statistics. The photon counts of the sources were 120 counts and 380 counts in the 0.5–2 keV and the 2–10 keV band, respectively, and the relative accuracy is estimated to be $\sim 15''$. Hence, we conclude that the peak position in the 0.5–2 keV band corresponds to another new soft X-ray source (here, the soft source), which was not found in the LSS due to lack of the photon statistics. Both of the sources are marked with crosses in Fig. 1 (a, b).

The nominal error of $1'$ for the absolute position of *ASCA*, is mainly affiliatable to a mis-alignment of the attitude sensors on the satellite base plate, coupled to a mis-match of the thermal expansion coefficient (Ueda et al. 1998b). We restored this temperature-dependent error using the on board house-keeping data, according to the method described in Ueda et al. (1998b). Finally, the peak positions for the soft and the LSS hardest source are determined to be (13h 15m 1.8s, $+31^\circ 42' 20''$) and (13h 15m 0.9s, $+31^\circ 41' 28''$), respectively, in the 2000 equinox with error circles of $0.5'$ radii (90% confidence level). Accordingly, they are designated as AX J131502+3142 and AX J131501+3141.

3.2. Spectra determined by the image analysis

Since the half power diameter of *ASCA* point spread function (PSF) is about $3'$, it is difficult to make individual spectra of these two sources separated by only $1'$. Hence, we extracted the energy spectra by analyzing images using the method described in Uno (1997). We made projected profiles of six different energy bands in the region illustrated in Fig. 1 (a, b) (dashed lines). Each energy band was selected to contain reasonable counts, at least 100 counts, for the profile fitting analysis as described below. We only used the data of SIS0 and SIS1 to construct the combined images, because the angular resolution of the SISs is better than that of the GISs. The projected axis was selected along a constant Right Ascension line which gives roughly the largest separation angle between the two sources. The profiles in the 0.5–2 keV and the 2–10 keV band are separately shown in Fig. 1 (c). We fitted these profiles with a model consisting of a background and two projected PSFs. The PSFs of XRTs were constructed by a ray-tracing program (Kunieda et al. 1995). The systematic error in the shapes of the PSFs is about 10% (Kunieda et al. 1995), which is much smaller than the statistical error. For the background, we used a model consisting of the CXB and the Non X-ray Background (NXB). The former was produced by the ray-tracing program and the latter was modeled from the night Earth data (Ueda 1996). In the fitting, we fixed the positions, but allowed the fluxes of the two sources to vary. Also the background level was varied. The best-fit fluxes of the two sources in the different energy bands give the energy spectra.

Using the energy spectra derived from the image fitting, we examined whether the spectral shapes were different between two observations, and found probable variability in the total flux for the AX J131501+3141 but found no significant change of the spectral shapes for both the sources. Therefore, to increase statistics, we summed the data of the two observations for the spectral analysis as is given in Fig. 2. Both the spectra of AX J131501+3141 and AX J131502+3142 were nicely fitted with a power-law with an absorption. The best-fit models and parameters are given in Fig. 2 and Table 1 (Methods A and B), respectively. Details of the analysis of the time variability are given in Sec.3.4.

3.3. The Mixed SIS/GIS Spectrum

To confirm the above results and even to make tighter constraints on the spectra of the two sources, we examined the spectra by an independent method. Firstly, we accumulated SIS0+1 spectrum in a $3'$ radius circle with the center at the peak of AX J131501+3141 for the summed data of the two observations. Since this spectrum inevitably contains photons from both of AX J131502+3142 and AX J131501+3141, separated only by $1'$, we refer the spectrum as the “Mixed SIS spectrum”. We subtracted the background taken from the region of the opposite corner in the same SIS chip after the correction for its position dependence in the detector plane (Ueda 1996). We constructed Auxiliary

Response Function (ARF) at the position of AX J131501+3141. The ARF at the position of AX J131502+3142 differs only by 4%, which is negligible in the present analysis.

Since we already found the presence of two power-law sources in the image-fitted spectra, we fitted the “Mixed SIS spectrum” with a model consisting of two power-laws with independent absorptions (two-power-law model), each of which represents AX J131502+3142 and AX J131501+3141. In the fitting, the power-law indices, normalizations, and column densities for both the components are allowed to be free parameters. The fitting result was found to be acceptable with the best-fit model and parameters given in Fig. 3 and Table 1 (Method C). We confirmed that the results obtained here are consistent with those obtained from the image-fitted spectra. Note that the spectral parameters for AX J131501+3141 ($\Gamma = 2.3_{-1.0}^{+1.3}$, $N_{\text{H}} = 7.9_{-3.4}^{+5.3} \times 10^{22} \text{ H cm}^{-2}$) are more tightly constrained, while no further constraint is given to AX J131502+3142.

Since GIS has higher efficiency in the high energy band than SIS, further constraints on the spectrum of AX J131501+3141 should be given by the GIS data. Thus, we made the GIS2+3 spectra from the summed image of the two observations within a 3' radius centered at the peak of AX J131501+3141. The background spectra were constructed from a 4'–6' radius annular region centered at the source. The background subtracted spectrum is given in Fig. 4 (a) (the “Mixed GIS spectrum”). Finally, to make the tightest constraints on the spectra, we fitted the Mixed GIS spectrum and the Mixed SIS spectrum simultaneously with a two-power-law model. The fitting was acceptable within 90% confidence level ($\chi^2/\text{d.o.f} = 22.5/16$). The best-fit parameters for the soft source AX J131502+3142 and the hard source AX J131501+3141 are $\Gamma_{\text{soft}} > -0.9$, $N_{\text{H,soft}} = 1.5_{-0.5}^{+1.1} \times 10^{22} \text{ H cm}^{-2}$, and $\Gamma_{\text{hard}} = 1.5_{-0.6}^{+0.7}$, $N_{\text{H,hard}} = 6.4_{-2.3}^{+3.1} \times 10^{22} \text{ H cm}^{-2}$, respectively. The best-fit models and parameters are given in Fig. 4 (a) and in Table 1 (Method D). Fig. 4 (b) shows two-parameter error contours for the photon index and the hydrogen column density of AX J131501+3141, obtained by the simultaneous fitting.

3.4. Time Variability

Since the spectral shapes of the two observations show no significant difference (see Sec.3.2), we fixed the best-fit model obtained with the Method D for both SIS and GIS spectra, and separately fitted the spectrum in each observation allowing only the normalization to vary. The best-fit fluxes are given in Table 2. While the flux of AX J131502+3142 did not change significantly, that of AX J131501+3141 increased by $29 \pm 17\%$ with a 90% statistical error in 0.5 year from the 1st to the 2nd observation.

4. Discussion

We extracted the accurate spectrum of the LSS hardest source, AX J131501+3141, taking account of the contamination from the nearby soft source, AX J131502+3142, from which no significant X-ray emission was found in the LSS (Ueda 1996). We found that AX J131501+3141 exhibits a large absorption of $N_H = (6_{-2}^{+4}) \times 10^{22}$ H cm⁻² with a photon index $\Gamma = 1.5_{-0.6}^{+0.7}$. It showed a long-term time variability between two observations separated by 0.5 year. While the photon index of AX J131501+3141 is consistent with the canonical value of type 1 AGNs (e.g., Mushotzky 1993), its absorption column density is larger than that of typical type 1 AGN by more than an order of magnitude, although a part of type 1 AGNs, about 10% of them (Schartel et al. 1997), shows a column density larger than 5×10^{22} H cm⁻².

It is important that this source is selected fully unbiasedly. Hence, its X-ray properties should provide a key to understand the general nature of the missing hard X-ray populations which constitute the CXB above 2 keV. Two major possibilities have been proposed to account for the apparent hard spectrum of the CXB: one is to introduce large absorptions of sources (e.g., Awaki 1991), and the other is to consider populations of sources with intrinsically flat spectra (e.g., Morisawa et al. 1990; Di Matteo & Fabian 1997). Our results of the LSS hardest source strongly suggest that highly absorbed sources play an important role in considering the origin of the hard X-ray background.

The large absorption of 6×10^{22} H cm⁻², the photon index of $\Gamma \sim 1.5$, and the time variability are common properties seen in type 2 Seyfert galaxies. In fact, systematic studies of type 2 Seyfert galaxies by Awaki et al. (1991) and Ueno (1996) revealed that they commonly show large absorptions of $\sim 10^{23}$ H cm⁻² and photon indices of 1.5–1.7. Akiyama et al. (1998) found one bright optical galaxy with $B = 17.25$ mag near the center of the X-ray error circle of 0.5' radius in the optical follow-up observations. No other optical source with the flux larger than $B = 22.4$ mag is found in the error circle. Akiyama et al. (1998) performed spectroscopic observations of the bright galaxy and found that ratios of emission lines are similar to those found in type 2 Seyfert galaxies. The redshift of this galaxy was determined to be 0.07. From the redshift, the observed flux in the 2–10 keV band, 5×10^{-13} erg cm⁻² s⁻¹, can be converted to the absorption corrected luminosity of $L_X \sim 2 \times 10^{43}$ erg s⁻¹. This luminosity is consistent with those of Seyfert galaxies. Thus, we identify AX J131501+3141 found in the unbiased X-ray survey as a type 2 Seyfert galaxy. Using the LogN-LogS relation in Hasinger et al. (1998), we estimate that the chance coincidence between AX J131501+3141 and AX J131502+3142 is $\sim 3\%$. However, these two sources have probably no physical correlation, because AX J131502+3142 is likely to be a QSO³ which is more distant than the new type 2 Seyfert AX J131501+3141.

³ In the optical imaging observations of R- and B-band by Akiyama et al. (1998), we found two point-like optical sources located at about 10'' north from the center of the error

Awaki (1991), Madau, Ghisellini & Fabian (1994) and Comastri et al. (1995) predicted that the combination of type 1 and type 2 AGNs can reproduce the CXB spectrum, based on the unified AGN scheme (e.g., Antonucci 1993). In the scheme, type 1 and type 2 AGNs are essentially the same objects, observed from different viewing angle. These type 2 AGNs, which exhibit apparently fainter and harder X-ray spectra than those of type 1 AGNs, should become detectable as the detector sensitivity increases. Although we have examined only one sample from the LSS at this moment, the result is encouraging not only for the unified AGN scheme, but also for solving the origin of the CXB.

The authors express their thanks all of the members of the *ASCA* team whose efforts made these observations and data analysis possible. We are grateful to H. Inoue for his valuable comments. We thank the referee, G. Hasinger, for his useful advice. M. S. thanks Y. Maeda for discussion. M. S. and M. A. acknowledge the supports from the Japan Society for the Promotion of Science for Young Scientists.

circle with $30''$ radius for the soft source (AX J131502+3142). They are very close to each other and their magnitudes are comparable. Total magnitudes of the two sources are B=20.8 mag and R=19.6 mag; B-R color is 1.21. Since both the optical color and the optical to soft X-ray flux is consistent with that for type-1 AGNs, it is possible that one of them is a quasar which is also responsible for AX J131502+3142. However there are fainter optical sources ($R_{\lesssim 22}$) in the error circle and the optical identification for AX J131502+3142 is not clear yet.

REFERENCES

- Akiyama, M., et al. 1998, ApJ, in press, astro-ph/9801173
- Antonucci, R. 1993, ARA&A, 31, 473
- Awaki, H. 1991, Ph.D. thesis, Nagoya Univ.
- Awaki, H., Koyama, K., Inoue, H., & Halpern, J. P. 1991, PASJ, 43, 195
- Burke, B. E., Mountain, R. W., Harrison, D. C., Bautz, M. W., Doty, J. P., Ricker, G. R., & Daniels, P. J. 1991, IEEE Trans. ED-38, 1069
- Burke, B. E., Mountain, R. W., Daniels, P. J., & Dolat, V. S. 1994, IEEE Trans. Nuc. Sci., 41, 375
- Comastri, A., Setti, G., Zamorani, G., & Hasinger, G. 1995, A&A, 296, 1
- Day, C., Arnaud, K., Ebisawa, K., Gotthelf, E., Ingham, J., Mukai, K., & White, N. 1995, The ABC Guide to *ASCA* Data Reduction, NASA/Goddard Space Flight Center
- Fabian, A. C., & Barcons, X. 1992, ARA&A, 30, 429
- Gendreau, K. C., et al. 1995, PASJ, 47, L5
- Giacconi, R., Gursky, H., Paolini, F. R., & Rossi, B. B. 1962, Phys. Rev. Lett., 9, 439
- Hasinger, G. 1996, A&AS, 120, 607
- Hasinger, G., Burg, R., Giacconi, R., Schmidt, M., Trümper, J., & Zamorani, G. 1998, A&A, 329, 482
- Inoue, H., Kii, T., Ogasaka, Y., Takahashi, T., & Ueda, Y. 1996, in proc. of “Röntgenstrahlung from the Universe”, eds. Zimmermann, H. U., Trümper, J., & Yorke, H., p323
- Kunieda, H., Furuzawa, A., Watanabe, M., & the *ASCA* XRT Team 1995, the *ASCA* News No.3, NASA/Goddard Space Flight Center, p3
- Madau, P., Ghisellini, G., & Fabian, A. C. 1994, MNRAS, 270, L17
- Makishima, K., et al. 1996, PASJ, 48, 171
- Di Matteo, T., & Fabian, A. C. 1997, MNRAS, 286, 393
- McHardy, I. M., et al. 1998, MNRAS, in press
- Morisawa, K., Matsuoka, M., Takahara, F., & Piro, L. 1990, A&A, 236, 299

- Mushotzky, R. F. 1993, *ARA&A*, 31, 717
- Ohashi, T., et al. 1996, *PASJ*, 48, 157
- Serlemitsos, P. J., et al. 1995, *PASJ*, 47, 105
- Schartel, N., Schmidt, M., Fink, H. H., Hasinger, G., & Trümper, J. 1997, *A&A*, 320, 696
- Tanaka, Y., Inoue, H., & Holt, S. S. 1994, *PASJ*, 46, L37
- Ueda, Y. 1996, Ph.D. thesis, Tokyo Univ.
- Ueda, Y., et al. 1998a, *Nature*, 391, 866
- Ueda, Y., et al. 1998b, will appear in *ASCA News*, NASA/Goddard Space Flight Center
- Ueno, S. 1996, Ph.D. thesis, Kyoto Univ.
- Uno, S. 1997, Ph.D. thesis, Gakusyuin Univ.
- Vikhlinin, A., Forman, W., Jones, C., & Murray, S. 1995, *ApJ*, 451, 553

Fig. 1.— (a, b) SIS0+1 image contours in the 2nd observation (1996 June). The coordinates are in J2000. Images are smoothed with Gaussian of $\sigma = 20$ pixels (~ 0.54 arcmin.). The contour levels are linearly spaced by ten lines from 0 to 2.0×10^{-3} c/s/16pixels and from 0 to 5.2×10^{-3} c/s/16pixels, for (a) the 0.5–2 keV and (b) the 2–10 keV band image, respectively. The peak positions corresponding to AX J131502+3142 and AX J131501+3141 are marked with crosses. (c) The projected profiles of the 0.5–2 keV and the 2–10 keV band in the region represented with dashed lines. The data represented with open circles and crosses correspond to that for the 0.5–2 keV and the 2–10 keV band data, respectively.

Fig. 2.— The SIS0+SIS1 spectra obtained with the image-fit. Both spectra are fitted with an absorbed power-law (Method A, B). (a) AX J131502+3142 (Soft source) (b) AX J131501+3141 (Hard source)

Fig. 3.— The mixed SIS spectrum with the best-fit of two-power-law model (Method C).

Fig. 4.— (a) Same as Fig.3 but for the GIS spectrum and the best-fit model in the simultaneous fitting (Method D) of SIS+GIS data. (b) The 68, 90, 99% confidence contours for the photon index and hydrogen column density of AX J131501+3141 in the simultaneous fitting of SIS+GIS data.

Table 1: The fitting results

Method ^a	AX J131502+3142 (Soft component)		AX J131501+3141 (Hard component)		$\chi^2/d.o.f.$
	Photon index	N_H (10^{22} H cm ⁻²)	Photon index	N_H (10^{22} H cm ⁻²)	
(A)	$3.8_{-2.6}^{>6}$	0.7 ± 2.4	2.5/3
(B)	$2.8_{-1.8}^{+2.7}$	11_{-6}^{+13}	2.6/3
(C)	> 1.3	$1.7_{-0.6}^{+1.0}$	$2.3_{-1.0}^{+1.3}$	$7.9_{-3.4}^{+5.3}$	4.3/4
(D)	> -0.9	$1.5_{-0.5}^{+1.1}$	$1.5_{-0.6}^{+0.7}$	$6.4_{-2.3}^{+3.1}$	22.5/16

^aDescription of the methods:

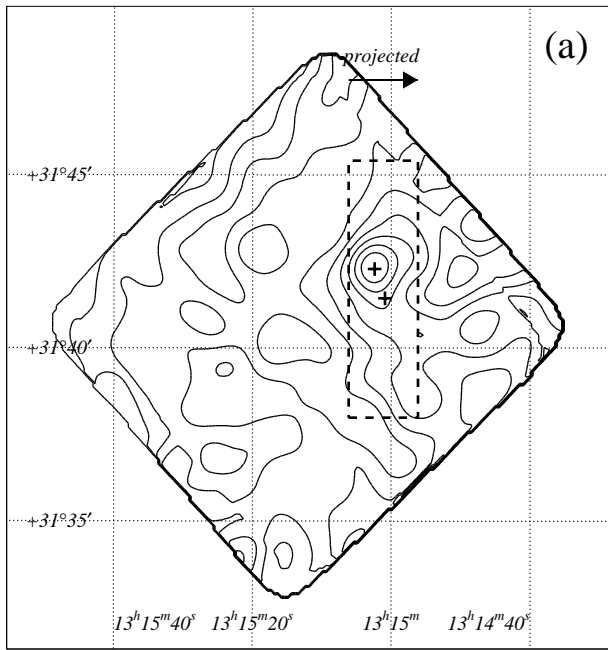
- (A) The SIS0+1 spectrum for the soft source AX J131502+3142 made with image-fitting. An absorbed power-law with all free parameters is used.
- (B) Same as (A), but for the hard source AX J131501+3141.
- (C) The mixed SIS Spectrum fitted with a two-component power-law model with absorption.
- (D) Same as the model (C) but for a combined fitting with SIS and GIS.

Table 2: The fluxes of AX J131502+3142 and AX J131501+3141

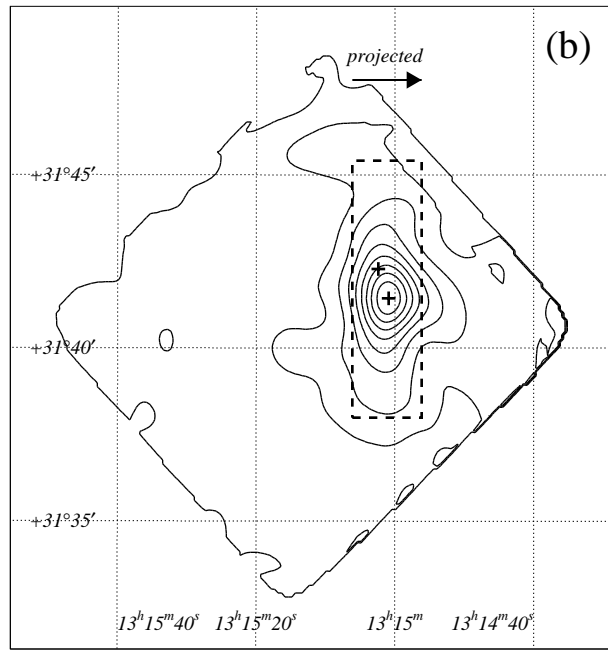
			1st epoch.	2nd epoch.
AX J131502+3142	(0.5–2 keV)	SIS	0.16 ± 0.08	0.23 ± 0.08
AX J131501+3141	(2–10 keV)	SIS	5.1 ± 0.8	6.7 ± 0.8
		GIS	4.5 ± 0.7	5.7 ± 0.7
		SIS+GIS ^a	4.8 ± 0.5	6.2 ± 0.5

Note. — Unit of flux is 10^{-13} erg cm⁻² s⁻¹. Each error is 90% confidence.

^aMean flux of AX J131501+3141 about SIS and GIS.



SIS0+1 (0.5-2keV)



SIS0+1 (2-10keV)

